

## PHOTODEGRADATION OF DYES RB-5 AND RL-6 USING $Fe_2O_3-TiO_2$ SEMICONDUCTORS

---

*Ana Karla Aguilera*

Tecnológico de Parral-TNM, Department of Industrial Engineering, Mexico

*Roman Ramirez Lopez*

Department of Basic Sciences, Higher School of Chemical Engineering and Extractive Industries, National Polytechnic Institute Lindavista, UPALM, Mexico.

*Raul Suarez Parra*

Institute of Renewable Energies, National Autonomous University of Mexico, Mexico

*Leonard Gonzalez Reyes*

Department of Basic Sciences, Autonomous Metropolitan University, Mexico

*Saul Holguin Quinones*

Department of Basic Sciences, Autonomous Metropolitan University, Mexico

*Anatolio Martinez Jimenez*

Department of Basic Sciences, Autonomous Metropolitan University, Mexico

*Isaiah Hernandez Perez*

Department of Basic Sciences, Autonomous Metropolitan University, Mexico.

<https://orcid.org/0000-0003-1607-3434>

All content in this magazine is licensed under a Creative Commons Attribution License. Attribution-Non-Commercial-Non-Derivatives 4.0 International (CC BY-NC-ND 4.0).



**Abstract:** In the present work, the photodegradation of Reactive Black Number 5 (RB-5) and Lanazol Red No 6 (RL-6) dyes was studied using modified TiO<sub>2</sub> semiconductors with 5, 10 and 20 wt% Fe<sub>2</sub>O<sub>3</sub>. The materials used were synthesized by the sonochemical method; To determine their physicochemical properties, the techniques of XRD, Scanning Electron Microscopy (SEM), RD-UV-Vis spectrophotometry and FTIR were used. Photoactivity studies were carried out in a batch reactor equipped with a cooling jacket, magnetic stirring, and UV or Vis lamps. The depth of degradation was monitored by UV-vis and total organic carbon analysis.

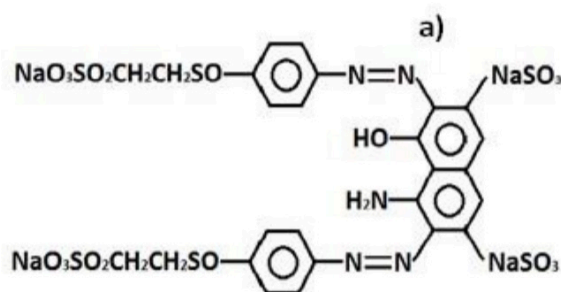
**Keywords:** Azo dyes, photodegradation, sonochemical synthesis, Fe<sub>2</sub>O<sub>3</sub>-TiO<sub>2</sub>.

## INTRODUCTION

The contamination of water resources by industries is an environmental problem worldwide, among the industries that consume the most fresh water are the paper and textile industries, generating large volumes of wastewater.[1]. According to UN data, it is estimated that the textile industry is responsible for at least 20% of global wastewater[two], these effluents are generally intense in color, with a high concentration of inorganic and organic compounds (some persistent), which are not easily degraded naturally[3]. The textile industry generates a large amount of polluting waste for the environment and high toxicity for living beings, which are discharged into different bodies of water (rivers, lakes, seas and oceans). Within the pollutants emitted by the textile industry, which have a great impact on the environment, there are mainly azo dyes, which, in addition to providing color to fabrics, due to their physical and chemical properties, present complex structures with high photochemical stability, chemical and biological; this represents a serious

contamination problem that cannot be solved through conventional water treatment processes [4]. Today these types of processes are inefficient for the removal of azo dyes, since several studies have reported on the mutagenicity of these dyes and their potential to cause cancer, both in its primary form and in the degradation process, since it can form highly toxic products for living beings [5-7]. Different investigations have shown that advanced oxidation processes (POA) are efficient in the degradation of persistent pollutants[8-11], particularly heterogeneous photocatalysis has which emerges as a promising process in wastewater treatment, since it is suitable for the elimination of aromatic molecules present in the structures of azo dyes and their potential danger to health.

RB-5 and RL-6 dyes are commonly used in the textile industry, representing a serious problem as a waste product in residual water, because a high percentage of this dye is not used during the dyeing process and is discarded to the drain; These dyes are characterized by having azo (-N=N-) and vinylsulfone (R-SO<sub>2</sub>-Ar) groups in their molecule, which give them high resistance and chemical and biological stability. Figure 1 shows the chemical structures of the dyes RB-5 and RL-6. According to the literature, these molecules are complex and therefore difficult to degrade by physical-chemical processes, so their removal represents a challenge from a scientific and technological point of view.



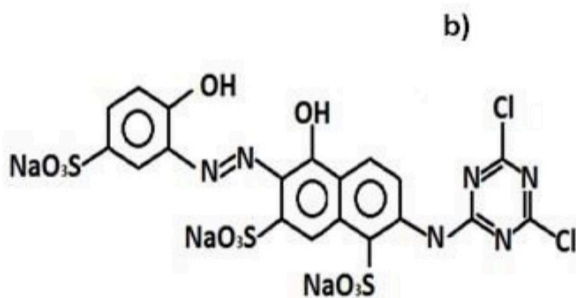


Figure 1. Molecules of azo-type dyes, a) RB-5) and b) RL-6

It has been shown that through photo-oxidation processes, using heterogeneous catalysts, it is possible to achieve organic contaminant removal efficiencies greater than 90% in short reaction times and under normal operating conditions. This process consists of the irradiation of a semiconductor material with visible or UV light, so that an electron from the valence band is promoted to the conduction band, generating the hole-electron pair, causing the decomposition of the organic contaminant with the  $h^+$ . While the electrons in the conduction band can react with the  $O_2$  adsorbed on the interface and generate superoxide radicals ( $O_2^{\bullet-}$ ), hydroperoxide radicals ( $HO_2^{\bullet}$ ) or photogenerate hydrogen peroxide ( $H_2O_2$ ), which are highly oxidizing agents, as can be seen in the scheme of Fig. 2.

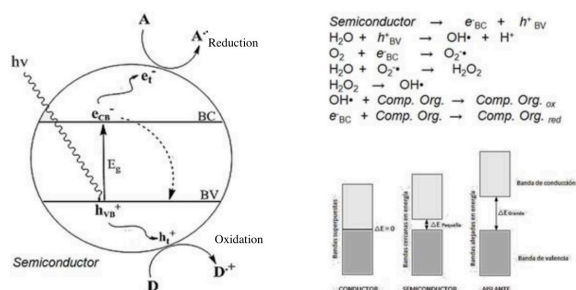


Figure 2. Scheme of a heterogeneous photocatalysis process.

TiO<sub>2</sub> is considered the photocatalyst par excellence, due to its wide bandwidth  $E_g = 3.2$  eV and its excellent photocatalytic

properties for the mineralization of organic compounds, however, its use is limited to light irradiation in the UV region, therefore, materials that improve the aforementioned properties are required. In the present work, the modifications of the structural, textural and opto-electronic properties are presented, incorporating Fe<sub>2</sub>O<sub>3</sub>, in the TiO<sub>2</sub> matrix at different concentrations, as well as the evaluation of its photocatalytic properties, using the degradation of textile dyes as a model reaction. RB-5 and RL-6.

## EXPERIMENTAL METHODOLOGY

All the materials were obtained by sonochemical (ultrasonic) synthesis, using a Cole Parmer 08895-40 ultrasonic bath, with a frequency of 40 KHz, an output power of 135 W and a voltage of 120 V. As precursors, tetra-Titanium isopropoxide (TIPT Aldrich 97%) and Ferric nitrate (JT Baker 97%). In a typical synthesis, 30 ml of TIPT solution in acetone-methanol are placed in a sonochemical reactor (40 KH, 135 W) for 10 minutes, then the necessary amount of an alcoholic solution of Fe (NO<sub>3</sub>)<sub>3</sub> 9 H<sub>2</sub>O is added. to obtain 0, 5, 10, 15 and 20% by weight of Fe<sub>2</sub>O<sub>3</sub>; the mixture was sonicated for another 50 min. Subsequently, the product is dried at 60 °C until the total elimination of the solvents in a rotary steam [12-14].

The materials were characterized by XRD (Philips Xpert, with Cu-K $\alpha$  radiation ( $\lambda = 0.15409$  nm), scanning speed of 0.02 °/s and operated at 45 kV and 40 mA), the crystallite size was determined by the Debye equation-Scherrer: [ ], UV-Vis spectrophotometry in diffuse reflectance mode (Varian-Cary IG, equipped with an integrating sphere, with MgO reference), the bandwidth ( $E_g$ ) was determined using the Tauc equation: and the Kubelka-Munk transformation (FR). FTIR spectroscopy using a Perkin Elmer Frontier instrument with a diamond tip attachment

(ATR) for powders and liquids was used to obtain the IR spectrum of TiO<sub>2</sub> and Fe<sub>2</sub>O<sub>3</sub>. Finally,  $D = \frac{K\lambda}{\beta \cos \theta} \alpha(h\nu)^{1/n} = B (h\nu - E_g)$

The photocatalytic evaluations were carried out in a batch reactor, equipped with a UV light source, with emission at  $\lambda_{max} = 365$  nm, using a volume of 200 mL of dye solution (RB-5 or RL-6) at an initial concentration of 100 ppm, with 0.05 g of photocatalyst at pH conditions = 3.2, 298 K and 77.99 KPa. The degradation of the dye was monitored by taking aliquots of the suspension at regular time intervals (20 minutes); by UV-Vis spectroscopy (Varian Cary I) for the RL-6 dye at 274 nm, 315 nm and 498 nm, and for the RB-5 at 274 nm, 315 nm and 598 nm; which are the wavelengths of the absorbance spectrum corresponding to the aromatic group ( $\lambda = 254$  nm), the azo group ( $\lambda = 315$  nm) and the chromophore ( $\lambda = 598$  nm), respectively.

## RESULTS

For the identification of phases and the calculation of the average crystal size, the X'Pert HighScore Plus software and the Scherrer equation were used. As references, pure samples of TiO<sub>2</sub> and Fe<sub>2</sub>O<sub>3</sub> were used, finding that unmodified TiO<sub>2</sub> present a mixture of anatase-rutile phases (80:20 respectively), due to the presence of characteristic reflections at 25 and 27°2 $\theta$ , while the pure Fe<sub>2</sub>O<sub>3</sub> sample presents a spectrum with low crystallinity (see insert of Fig. 4) related to the hematite phase (with localized reflections at 33 and 35 °2 $\theta$ ). For the Fe<sub>2</sub>O<sub>3</sub> modified samples, it is observed that, as the iron oxide content increases, the samples lose crystallinity, which can be attributed to an inhibitory effect of Fe when incorporated into the TiO<sub>2</sub> structure, as can be seen in the diffraction patterns of Figure 4. Additionally, it is important to point out that the average crystal size of the different

synthesized semiconductors and used in the photodegradation of the RB-5 and RL-6 dyes decreases with the Fe content, as shown in the results of Table 1.

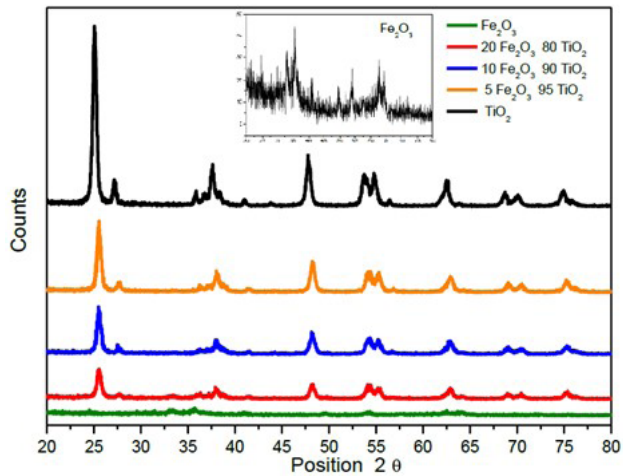
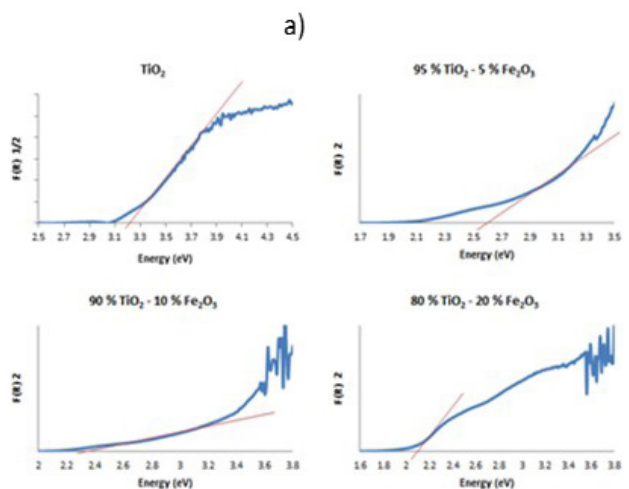


Figure 4.- Diffraction patterns of TiO<sub>2</sub> samples and their modifications with Fe<sub>2</sub>O<sub>3</sub>

From the results of RD-UV it was found that the materials are within the group of semiconductors and that the energy of the forbidden band ( $E_g$ ), increases with the increase of the Fe content, this may be due to the formation of states interband electrons close to the conduction band of TiO<sub>2</sub>, as can be seen in Fig. % and Table 1.



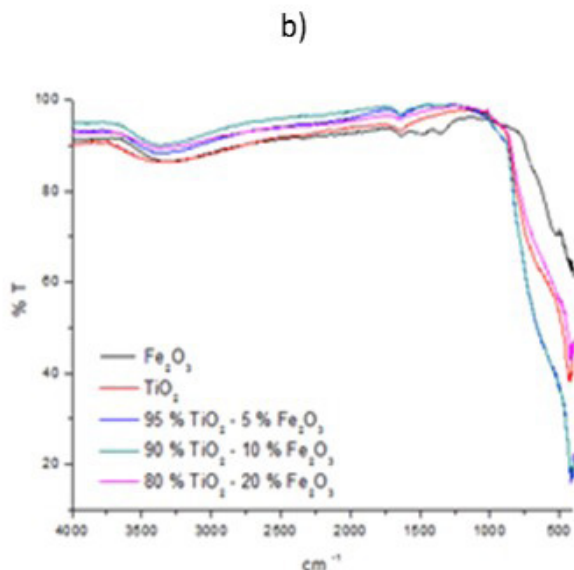


Figure 5.- a) RD-UV-Vis spectra and b) FTIR of the different synthesized materials.

On the other hand, from the FTIR results, a broad band at approximately 3200 cm<sup>-1</sup> is observed in all the samples, characteristic of the OH groups (moisture in the materials); an intense band between 500 - 400 cm<sup>-1</sup> is also observed in all the materials, due to the interaction of the O - M<sup>+</sup> bonds (associated with metal oxides); a low intensity vibration band is also observed near 1650 cm<sup>-1</sup>, characteristic of TiO<sub>2</sub>, which is maintained after incorporating Fe<sub>2</sub>O<sub>3</sub>, finally, the vibration bands characteristic of Fe<sub>2</sub>O<sub>3</sub>, located at 1200 - 1300 cm<sup>-1</sup> are not observed after incorporation into the TiO<sub>2</sub> structure, as can be seen in Figure 5b.

From the scanning electron microscopy micrographs, irregular porous morphologies are observed both in their shape and size, which is important for the photocatalytic adsorption and transformation processes, it is also evident that the roughness of the surface is due to largely due to the fact that particles with sizes less than 400 nm aggregate irregularly to structures with sizes greater than 1.5 μm, possibly due to growth controlled by some diffusive process. Fig. 6, 5

shows a general view of the 5% Fe<sub>2</sub>O<sub>3</sub> - 95% TiO<sub>2</sub> sample as a whole, where a uniform distribution of the photocatalyst components is evident.

Based on the photoactivity tests, considering that the reactions were carried out in an acid medium, it was found that it is possible to achieve discoloration and a total decrease after 180 minutes of reaction; It is also observed that modifying the TiO<sub>2</sub> matrix with Fe<sub>2</sub>O<sub>3</sub> improves the photocatalytic properties. For the reaction conditions used during this experimentation, the semiconductor with 95%TiO<sub>2</sub> -5%Fe<sub>2</sub>O<sub>3</sub>, is the one that presents the best degradation performance, as can be seen in the results of Table 2.

From Table 2, it is observed that an increase in the Fe content decreases the photoactivity, highlighting the influence not only of the crystal size, but also of the band width of the synthesized materials, that is, for the TiO<sub>2</sub> materials. - Fe<sub>2</sub>O<sub>3</sub> photoactivity is favored at larger crystal sizes, and lower E<sub>g</sub>, this can be attributed to the saturation of the interband states generated by the incorporation of Fe<sub>2</sub>O<sub>3</sub>, within the TiO<sub>2</sub> matrix. In order to find a kinetic model that describes the performance of the semiconductor 95%TiO<sub>2</sub>-5% Fe<sub>2</sub>O<sub>3</sub>, experiments were carried out varying the concentrations of the dyes in a range from 20 to 100 ppm, using the most favorable reaction conditions (pH = 3, mass of semiconductor = 0.05g and 0.02 ml of H<sub>2</sub>O<sub>2</sub>), as well as the Langmuir-Hinshelwood (LH) equation;  $-r = \frac{kK C}{1+K C} I = I_0 \times 10^{-\epsilon R}$ .

Fig.7 shows the results of the kinetic analysis carried out for the dyes RB-5 and RL-6, finding that the photodegradation of RB-5 can be adequately described by integrating a model of pseudo first order (se considered, that the steady state, the denominator of the LH equation is constant), while for the RL-6 dye, the performance is better described by integrating the differential equation of

Material	Principal Reflection (2 $\theta$ )	Reflection Secondary ((2 $\theta$ ))	FWHM	Crystal size (nm)	Energy (eV)
TiO <sub>2</sub>	25,119	27,237	0.433	25	3.21
Fe <sub>2</sub> O <sub>3</sub>	35,761	33,181	0.22	5	1.74
95% TiO <sub>2</sub> - 5% Fe <sub>2</sub> O <sub>3</sub>	25,537	27,712	0.394	22	2.2
90% TiO <sub>2</sub> - 10% Fe <sub>2</sub> O <sub>3</sub>	25,502	27,653	0.354	17	2.43
80% TiO <sub>2</sub> - 20% Fe <sub>2</sub> O <sub>3</sub>	25,509	27,785	0.551	13	2.75

Table 1. Average crystal sizes and bandgap energy of the different catalysts.

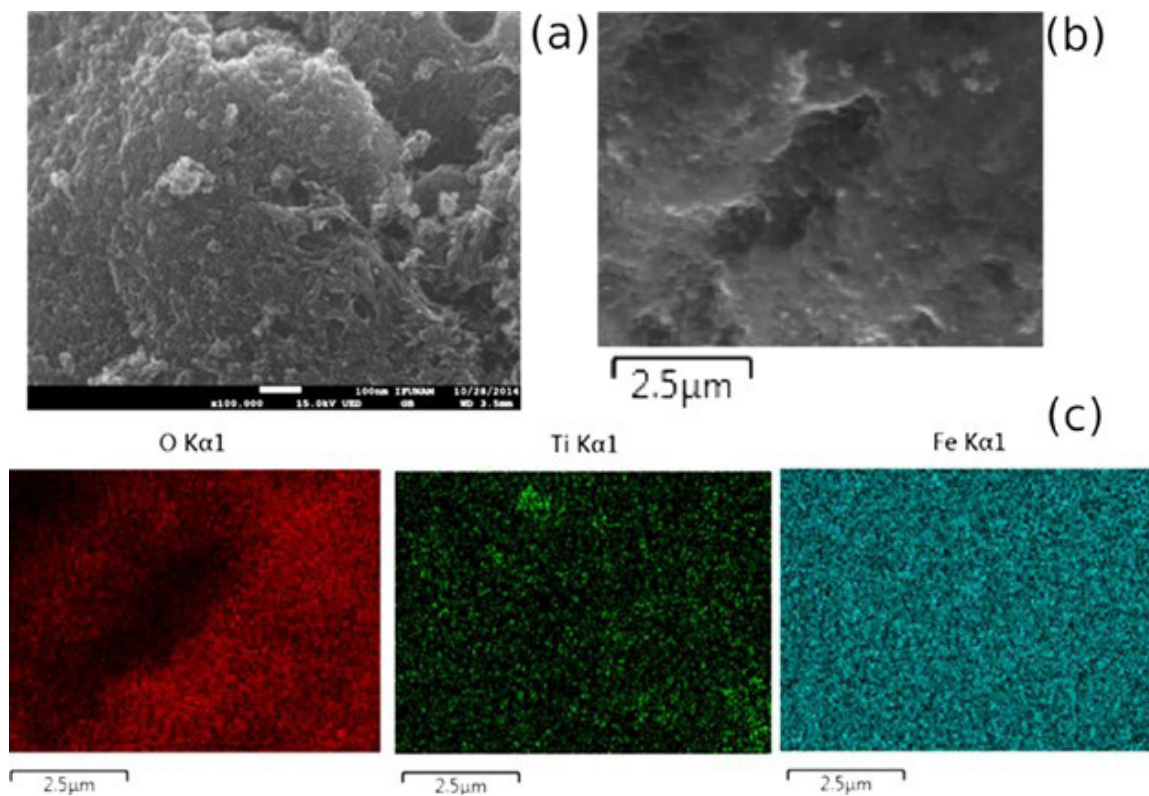


Figure 6.- Morphology and SEM, elemental distribution mapping for the sample 5% Fe<sub>2</sub>O<sub>3</sub> - 95% TiO<sub>2</sub>.

RB-5 degradation*	
Material	Photodegradation (%)
TiO <sub>2</sub>	84.15
Fe <sub>2</sub> O <sub>3</sub>	85.85
95% TiO <sub>2</sub> - 5% Fe <sub>2</sub> O <sub>3</sub>	99.17
90% TiO <sub>2</sub> - 10% Fe <sub>2</sub> O <sub>3</sub>	95.25
80% TiO <sub>2</sub> - 20% Fe <sub>2</sub> O <sub>3</sub>	90.16

RL-6 degradation*	
Material	Photodegradation (%)
TiO <sub>2</sub>	85.95
Fe <sub>2</sub> O <sub>3</sub>	86.61
95% TiO <sub>2</sub> - 5% Fe <sub>2</sub> O <sub>3</sub>	99.53
90% TiO <sub>2</sub> - 10% Fe <sub>2</sub> O <sub>3</sub>	96.84
80% TiO <sub>2</sub> - 20% Fe <sub>2</sub> O <sub>3</sub>	92.41

\*Reaction conditions pH = 3, 0.05g of 5%Fe<sub>2</sub>O<sub>3</sub>- TiO<sub>2</sub>, 100 ppm of dye, 0.02 ml of H<sub>2</sub>O<sub>2</sub> and Visible light

Table 2 Photocatalytic performance of the synthesized materials

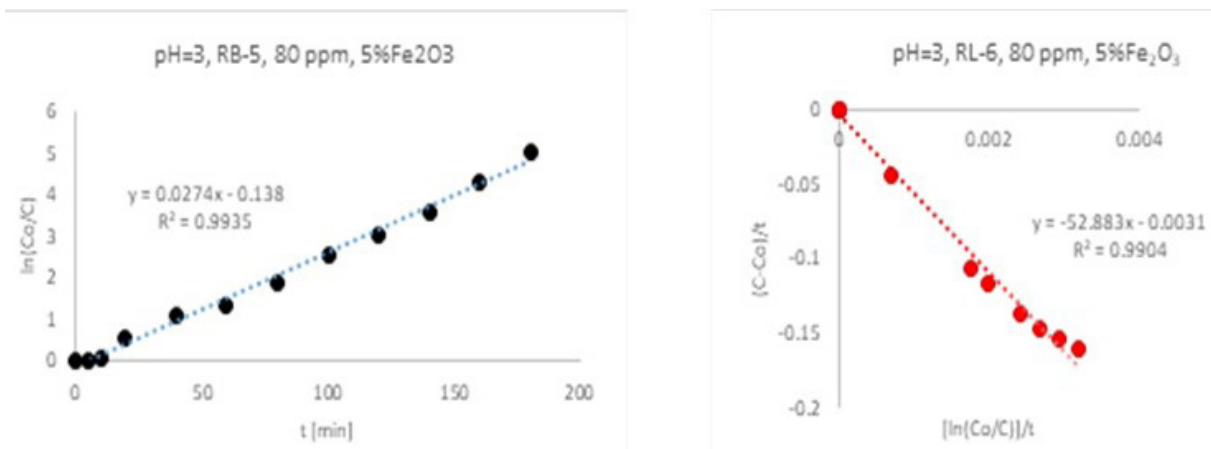


Fig. 7 Kinetic behavior of the photodegradation of the dyes RB-5 and RL-6.

the Langmuir-Hinshelwood model. It is important to mention that in both cases a good correlation ( $R > 0.99$ ) was found between the experimental results and the model proposed for each case.  $-r = k''CI + KC$ .

## CONCLUSIONS

The sonochemical synthesis method allows obtaining semiconductor materials with controlled photocatalytic properties with different TiO<sub>2</sub>:Fe<sub>2</sub>O<sub>3</sub> ratios, capable of decolorizing and mineralizing azo-type dyes, which are highly refractory to conventional water treatment processes. The incorporation of Fe to TiO<sub>2</sub> allows a better photocatalytic performance. The origin of the photoactivity in the visible region can be attributed to the electronic transitions of the "d" orbitals of iron towards titanium, as well as the formation of electronic states in the forbidden region (close to the conduction band) induced by the defects (oxygen vacancies), as well as a greater separation of the charges (the reduction in the e<sup>-</sup> - h<sup>+</sup> recombination processes) and not actually the decrease in Eg.

## THANKS

The authors appreciate the support received from the Department of Basic Sciences UAM-A, ESIQIE-IPN and the Institute of Renewable Energies-UNAM. Likewise, the technical support of Mario Rocha Pérez and Rogelio Morán Elvira

## REFERENCES

1. Prihod'ko R.V., Soboleva N.M., "Photocatalysis: Oxidative Processes in Water Treatment". *Journal of Chemistry*, 2013 p. 8.
2. Sakkas V. A., Islam M. A., Stalikas C., Albanis T.A., "Photocatalytic degradation using design of experiments: A review and example of the Congo red degradation", *J. of Hazardous Mater.*, Vol. 175, 2010, p. 33–44.
3. Lucas Marco S, "Degradation of the azo dye Reactive Black 5 by Fenton and photo-Fenton oxidation", *Dyes and Pigments*, Vol. 71, 2006, p. 236-244.
4. Venkataraman K., "The Chemistry of Synthetic Dyes. Reactive Dyes" *Academic Press* 1972.
5. Zhang, L., "Kinetics and mechanisms of charge transfer processes in photocatalytic systems" *Journal of Photochemistry and Photobiology, Photochemistry Reviews*, Vol.13, 2012, p. 263-276.
6. Kaur, J. and S. Singhal, "Facile synthesis of ZnO and transition metal doped ZnO nanoparticles for the photocatalytic degradation of Methyl Orange." *Ceramics International*, Vol. 40 (5), 2014, p. 7417-7424.
7. Ying-Chien C., Chin-Yu C., "Degradation of azo dye reactive violet 5 by TiO<sub>2</sub> photocatalysis", *Environmental Chemical Letter*, Vol. 7, 2011, p. 347-352.
8. Palanisami, B., Babu, C. M., Sundaravel, B., Anandan, S., Murugesan, V. (2013). Sol-Gel Synthesis of Mesoporous Mixed Fe<sub>2</sub>O<sub>3</sub>/TiO<sub>2</sub> Photocatalyst. *Journal of Hazardous Materials*, 233-244
9. Ibrahim, G.U., Halim, A.A. (2008). *Heterogeneous Photocatalytic Degradation of Inorganic Contaminants Over Titanium Dioxide: A Review of Fundamentals, Progress and Problems.* *Journal of Photochemistry and Photobiology C: Photochemistry Review*, 1-12.
10. Sengil. I.A., Ozacar, M. (2009). *The decolorization of C.I. Reactive Black 5 in aqueous solution by electrocoagulation using sacrificial iron electrodes.* *Journal of Hazardous Materials*. 161, 1369-1376.
11. Perkowitz, S. (1993). *Optical Characterization of Semiconductors: Infrared, Raman and Photoluminescence Spectroscopy.* Academic Press London.
12. González Reyes L., Hernández Pérez I., Robles Hernández F.C., "Effect of coarsening of sonochemical synthesized anatase on BET surface characteristics", *Chemical Engineering Science* Vol. 66, 2011, p. 721–728.
13. Xu, N., Shi, Z., Fan, Y., Dong, J., Shi, J., Hu, M. Z. C. (1999). *Effects of particle size of TiO<sub>2</sub> on photocatalytic degradation of methylene blue in aqueous suspensions.* *Industrial and Engineering Chemistry Research*, 38, 373–379.
14. M. May-Lozano, G. M. Ramos-Reyes, R. López-Medina, S. A. Martínez-Delgado, J. Flores-Moreno, I. Hernández-Pérez, "Effect of the Amount of Water in the Synthesis of B-TiO<sub>2</sub>: Orange II Photodegradation", *International Journal of Photochemistry*, 2014, p. 1–8.
15. E. Montiel-Palacios, A. K. Medina, C. Sampieri, C. Angeles, I. Hernandez-Perez, and R. Suarez-Parra, "Photo-catalysis of phenol derivatives whit Fe<sub>3</sub>O<sub>3</sub> nanoparticles dispersed on SBA-15," vol. 10, no. 4, pp. 548–552, 2009.